

SEDIMENTARY AND HYDRODYNAMIC PROCESSES OF TIDAL BORES: SILTATION OF THE ARCINS CHANNEL, GARONNE RIVER (FRANCE)

DAVID REUNGOAT⁽¹⁾, XINQIAN LENG⁽²⁾ & HUBERT CHANSON⁽³⁾

⁽¹⁾ *Université de Bordeaux, I2M, Laboratoire TREFLE, Pessac, France, d.reungoat@i2m.u-bordeaux1.fr*

⁽²⁾ *The University of Queensland, School of Civil Engineering, Brisbane QLD 4072, Australia, xinqian.leng@uqconnect.edu.au*

⁽³⁾ *The University of Queensland, School of Civil Engineering, Brisbane QLD 4072, Australia, h.chanson@uq.edu.au*

ABSTRACT

A tidal bore is a hydraulic jump in translation propagating upstream in an estuarine channel when a macro-tidal flood tide enters a funnel shaped river mouth with shallow waters. The tidal bore of the Garonne River (France) was extensively investigated in the Arcins channel in 2015, with a focus on the temporal evolution of hydrodynamics and sediment processes during a spring tide period. The tidal bore had a marked effect on the velocity field, including a rapid flow deceleration and flow reversal. Maximum flow deceleration between -0.65 m/s^2 to almost -1.4 m/s^2 were observed. The early flood flow motion was very energetic with large fluctuations of all velocity components. The suspended sediment concentration (SSC) data showed very large instantaneous SSC levels, in excess of 100 kg/m^3 , during the passage of the tidal bore front, as well as large SSCs during the first hour of the flood tide for all the entire observations. The work culminates a 5-year research project at the same site, showing a progressive siltation of the Arcins channel during the last three years.

Keywords: Tidal bores, Field measurements, Suspended sediment processes, Channel siltation, Garonne River

1 INTRODUCTION

A tidal bore is a compressive wave of tidal origin, which propagates upstream as the tidal flow turns to rising. It might be observed when a macro-tidal flood tide enters a funnel shaped river mouth with shallow waters (Tricker, 1965; Chanson, 2011). A related application is the tsunami-induced bore propagating in rivers (Tanaka et al., 2012). The occurrence of tidal and tsunami-induced bores has a significant impact on the natural systems. Their impact on sedimentary processes was documented in the field and in laboratory (Faas, 1995; Khezri and Chanson, 2015). It is understood that the bore propagation is associated with intense scouring and suspension of bed materials (Greb and Archer, 2007; Furgerot et al., 2016) (Fig. 1A). In cohesive sediment river systems, the erosional processes may be linked to the rheological properties of sediment deposits, and field observations suggest that the bore passage induces immediately some surface erosion followed by delayed bulk erosion (Faas, 1995; Keevil et al., 2015).

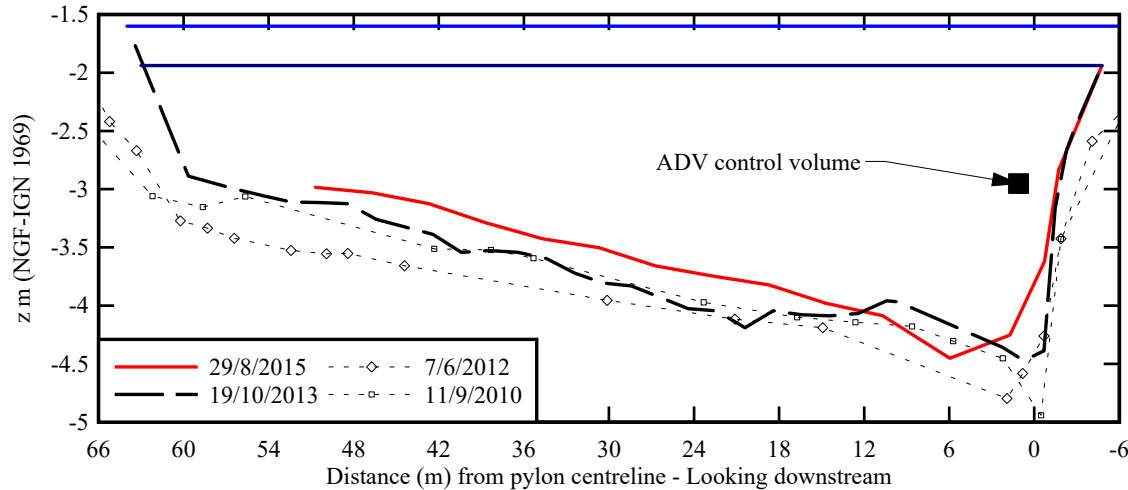
Herein new field measurements were repeated systematically at the same site in the Garonne River (France) on 29 August, 30 August, 31 August and 1 September 2015 and on 27 October 2015. Instantaneous velocity measurements were performed continuously at high-frequency (200 Hz) prior to, during and after each afternoon tidal bore. Instantaneous sediment concentration and suspended sediment flux data were derived from careful calibration of acoustic backscatter and checked against water sample concentrations.

2 INVESTIGATION SITE, INSTRUMENTATION AND METHODOLOGY

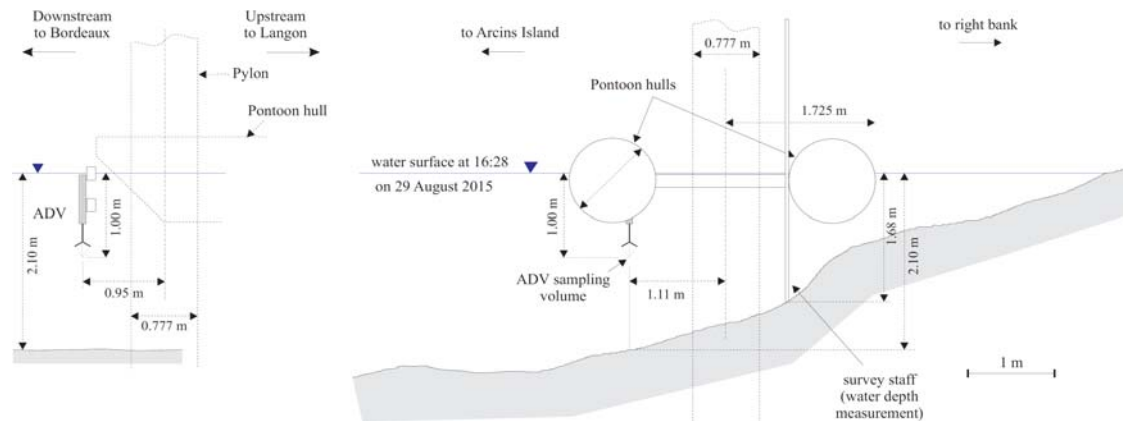
Field measurements were performed in the tidal bore of the Garonne River in the Arcins channel, close to Lastrene (France), at a site previously used (Chanson et al., 2011; Reungoat et al., 2014; Keevil et al., 2015). The Arcins channel is 1.8 km long, 70 m wide and about 1.1 to 2.5 m deep at low tide, between the Arcins Island and the right bank (Fig. 1A). The bathymetric data indicated a progressive siltation of the Arcins channel at the sampling site between 2012 and 2015 (Fig. 1B). Although the tides are semi-diurnal, the tidal data indicated slightly different periods and amplitudes typical of diurnal inequality. Detailed field measurements were conducted under spring tide conditions between 29 August and 1 September 2015, and on 27 October 2015, while additional observations were performed on 28 August 2015, 26 October and 28 October 2015. The tidal range was between 5.85 m to 6.32 m, and the tidal bore Froude numbers between 1.18 and 1.7 (Reungoat et al., 2016). All measurements were started prior to the passage of the tidal bore and ended at least one hour after the bore passage.



(A) Looking downstream on 28 October 2015 - The ADV unit was fixed to the pontoon next to the right bank



(B) Surveyed cross-section on 29 August 2015 with the initial water level (dark blue line), conjugate water depth (blue line) and ADV control volume - Comparison with the surveyed data in 2013, 2012 and 2010



(C) Un-distorted dimensioned sketch of the ADV mounting and sampling location relative to the bed and free-surface about 2 minutes prior to the tidal bore passage on 29 August 2015

Figure 1. Tidal bore investigation site in the Arcins channel, Garonne River (France) in August-October 2015

Free surface elevations were recorded continuously using a survey staff, while instantaneous velocity components were measured using a NortekTM ADV Vectrino+ equipped with a down-looking head. The ADV unit was fixed beneath a heavy pontoon and its control volume was located 1.0 m below the free-surface (Fig. 1). The ADV power setting (High- or Low) was selected after preliminary tests, to optimise the acoustic backscatter response of the ADV unit with the Garonne River sediment (Reungoat et al. 2016). The ADV system was sampled continuously at 200 Hz. The velocity signal post-processing included the removal of communication errors, the removal of average signal to noise ratio (SNR) data less than 5 dB, the removal of average correlation values less than 60% and despiking using the phase-space thresholding technique (Goring and Nikora, 2002; Wahl, 2003). The percentage of good samples ranged between 60 and 90% for the entire data sets.

Garonne River bed materials were collected at the end of ebb tide, next to the right bank. The soil sample consisted of soft cohesive mud and silty materials. A series of laboratory tests were conducted to characterise the particle size distribution, rheometry and backscatter properties. Water samples were also collected prior to

and shortly after the tidal bore about 0.2 m below the water surface. The water samples were dried in an oven, set at 40 C, to measure the mass of dry sediments and the sample sediment concentration. Further details are reported in Reungoat et al. (2016).

3 BASIC FLOW PATTERNS

3.1 Free-surface observations

On 28 August 2015 afternoon, no tidal bore was observed. On 29, 30 and 31 August, 1 September and 27 October 2015, the tidal bore formed at the downstream end of the Arcins channel. The bore extended rapidly across the entire channel width as a breaking bore in this very shallow region. The tidal bore was undular at the sampling location further upstream, although it was breaking close to the left bank (Fig. 1A). While the bore was undular, the free-surface elevation rose very rapidly during the bore passage: i.e., by 0.3 m to 0.5 m in the first 10 s. The tidal bore propagated up to the upstream end of the channel for the entire channel length. The bore passage was always followed by a series of strong whelps lasting for several minutes, with a wave period about 1 s (Fig. 2). For all field studies, the whelps were observed between one to three minutes after passage of the bore. In August-September, the free-surface wave motion was seen about three minutes after the front. In October, these whelps were seen about a minute after the bore front: that is, with a delay comparable to that observed in October 2013 at the same site. Figure 2 illustrates the well-formed whelp motion on 27 October 2015. The water depth data showed large free-surface fluctuations with a period about 1.3 to 1.5 s between 56270 s and 56310 s (Fig. 2B).

The tidal bore shape was characterised its Froude number $Fr_1 = (V_1+U)/(g \times A_1/B_1)^{0.5}$, where V_1 is the initial flow velocity positive downstream, U is the bore celerity positive upstream, g is the gravity acceleration, A_1 is the initial flow cross-section area and B_1 is the initial free-surface width, which were derived from bathymetric surveys conducted daily. The Froude number ranged from 1.2 to 1.7, consistent with the undular nature of the bore, except on 31 August 2015. On 31 August 2015, the bore front was undular on the channel centreline and towards to the right bank, but breaking close to the left bank. For the secondary waves, the relationships between Froude number, and dimensionless wave amplitude and wave length data, followed closely past field and laboratory observations and the results were close to a solution of the Boussinesq equation. During the late ebb tide, the current velocity decreased in the Arcins channel with time. The tidal bore had a marked effect on the velocity field (see below), with a rapid flow deceleration and flow reversal during the bore passage.

The application of the equations of conservation of mass and momentum in their integral form gives an analytical solution of the conjugate flow properties, namely the ratio of conjugate cross-section areas as a function of the Froude number and cross-section shape (Chanson, 2012). It yields:

$$\frac{A_2}{A_1} = \frac{1}{2} \times \frac{\sqrt{\left(2 - \frac{B'}{B}\right)^2 + 8 \times \frac{B}{B_1} \times Fr_1^2} - \left(2 - \frac{B'}{B}\right)}{\frac{B'}{B}} \quad [1]$$

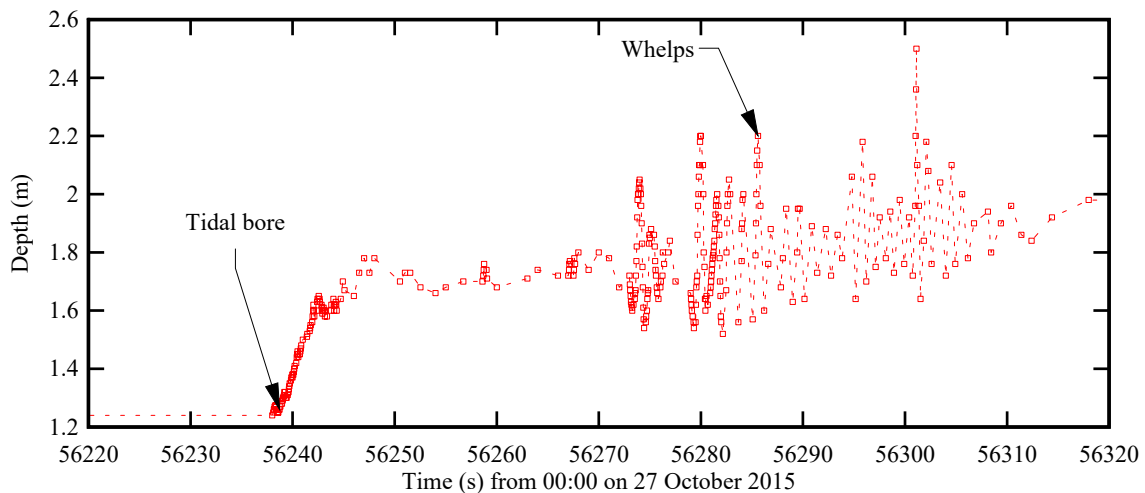
where A_2 is the new cross-sections area: $A_2 = A_1 + \Delta A$ (Fig. 3A), and B and B' are characteristic widths defined based upon the cross-sectional shape (Chanson, 2012). The present observations are reported in Figure 3B and Table 1 in terms of the ratio of conjugate cross-section areas A_2/A_1 as a function of the Froude number Fr_1 . The present data (filled square symbols) are compared with the momentum principle solution (Eq. (1)) (open circles) and previous field data (solid symbols) (Fig. 3B). For completeness, the Bélanger equation developed for a smooth rectangular channel is included (thin solid line). Figure 3B shows a good agreement between Equation (1) and the field data. It highlights further the improper application of the Bélanger equation in natural irregular-cross-sectional channels.

Table 1. Tidal bore properties at the sampling location during the 2015 field measurements in the Arcins channel (Garonne River, France)

DATE	Fr_1	U (m/s)	d_1 (m)	A_1 (m ²)	B_1 (m)	Δd (m)	A_1/B_1	B_2/B_1	B/B_1	B'/B_1	A_2/A_1
29/08/2015	1.18	4.23	1.685	101.4	67.6	0.338	1.50	1.034	1.019	1.012	1.23
30/08/2015	1.34	4.25	1.25	72.8	64.3	0.470	1.13	1.048	1.017	1.019	1.42
31/08/2015	1.70	4.79	1.122	56.6	65.1	0.496	0.87	1.068	1.032	1.025	1.59
01/09/2015	1.38	4.45	1.28	74.9	64.5	0.440	1.16	1.048	1.024	1.017	1.39
27/10/2015	1.33	4.61	1.24	88.0	65.9	0.480	1.34	1.049	1.019	1.017	1.37



(A) View from the right bank looking downstream about 30 s after the bore passage - Arrow points to whelps



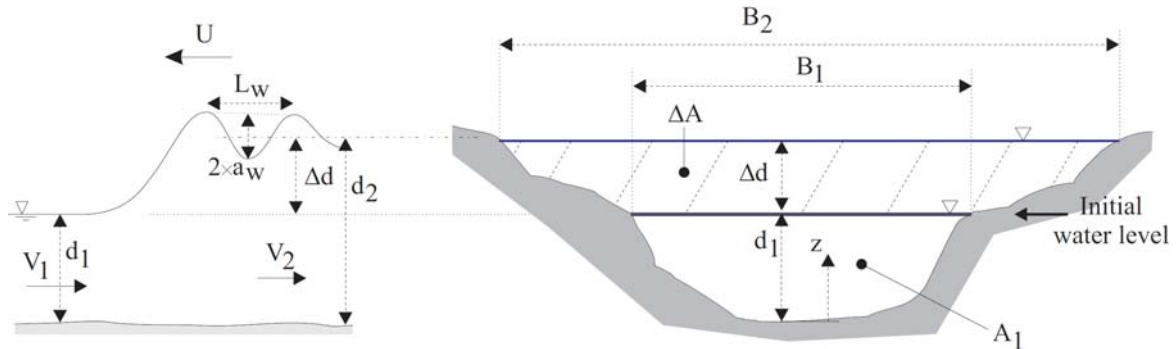
(B) Water depth observations at the survey staff

Figure 2. Well-formed whelp motion observed about a minute after tidal bore passage on 27 October 2015

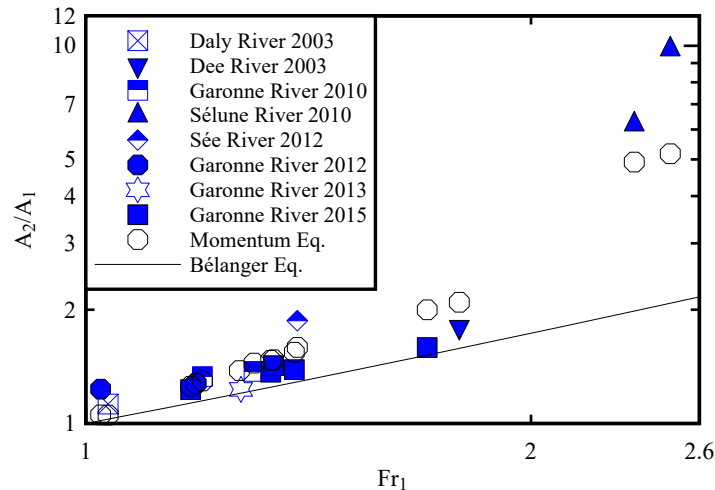
3.2 Velocity measurements

Velocity measurements were conducted continuously at high frequency prior to, during and after the tidal bore. Figure 4 shows a typical data set, where the longitudinal velocity component V_x is positive downstream, the transverse velocity component V_y is positive towards the left bank, and the vertical velocity component V_z is positive upwards. In Figure 4A, the time-variations of the water depth are included as well as surface velocity data on the channel centre. During the late ebb tide, the current velocity in the Arcins channel decreased with time. Immediately prior to the bore, the surface velocity dropped down to +0.2 m/s to +0.3 m/s at the channel centre. Lower instantaneous velocities were recorded by the ADV unit close to the left bank. The tidal bore occurrence had a marked effect on the velocity field, as illustrated in Figure 4. Namely a rapid flow deceleration and flow reversal were observed during the bore passage, followed by large and rapid fluctuations of all velocity fluctuations during the early flood tide. The maximum flow deceleration ranged from -0.65 m/s^2 to less than -1.4 m/s^2 (Table 2). A number of data are summarised in Table 2, regrouping basic flow properties prior to the bore (a couple of minutes prior to the bore), as well as flow properties recorded during the very early flood tide (i.e. 20 s after bore passage), early flood tide free-surface wave motion period, and flood tide (i.e. one hour after bore passage).

The bore passage was associated with large fluctuations of all velocity components, lasting throughout the flood tide. The flood flow was very energetic. About 100 s to 300 s after the bore front, some strong free-surface oscillation motion was observed (Fig. 3), associated with large oscillations of both horizontal and vertical velocity components with periods about 1.3 s to 1.5 s (Table 2). Such velocity oscillations were closely linked to the free-surface curvature and its induced vertical motion.



(A) Definition sketch of a tidal bore propagating in a natural irregular-cross-sectional channel

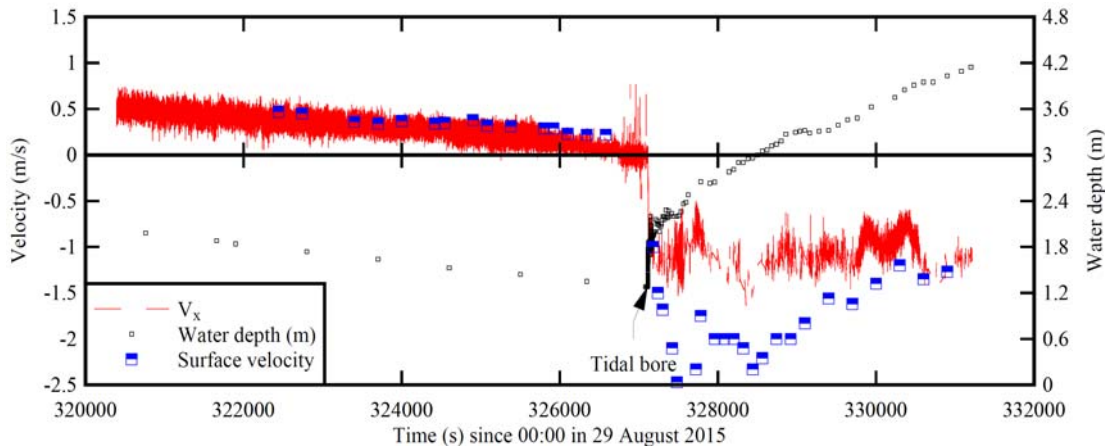


(B) Relationship between conjugate cross-sectional area ratio A_2/A_1 and Froude number Fr_1 in tidal bores - Comparison between field observations (blue symbols), momentum principle solution (Eq. (1), black hollow circles) and the Bélanger equation (thin solid line)

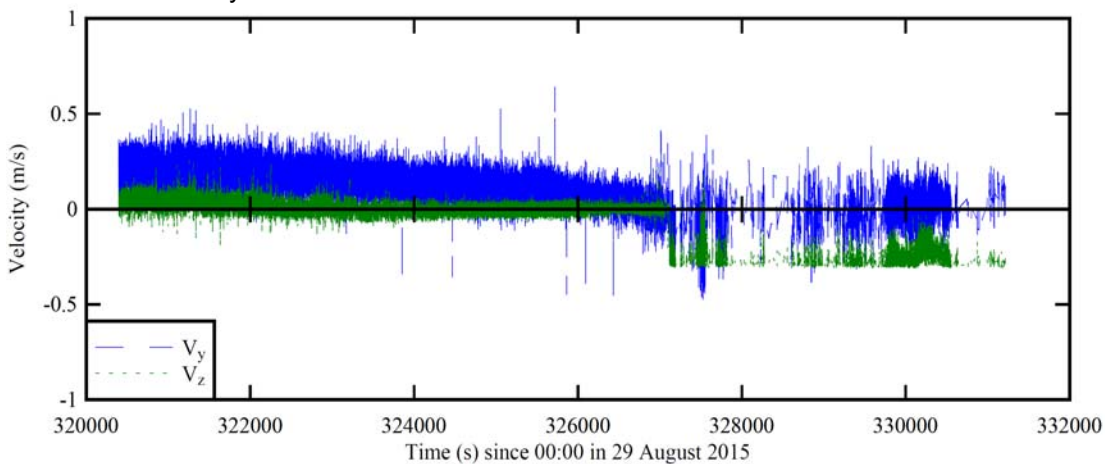
Figure 3. Free-surface characteristics of the tidal bore of the Garonne River at Arcins in August, September and October 2015 - Comparison with past field observations

The turbulent properties were estimated both before and after the tidal bore passage. A few basic characteristics are summarised in Table 2. After the rapid deceleration, the present data showed large velocity fluctuations during the very-early flood tide, as first reported by Chanson et al. (2011). Dimensionless velocity fluctuations $v'/|\bar{V}_x|$ ranged from 10% to 30% for all velocity components then, where v' is the standard deviation of a velocity component and $|\bar{V}_x|$ is the magnitude of time-averaged longitudinal velocity. Typical data are illustrated in Figure 4 with the tidal bore passage about $t \sim 327,550$ s, and quantitative observations are reported in Table 2.

The velocity fluctuations were large during the flood tide and large fluctuations were recorded for the first two hours. For example, dimensionless velocity fluctuations $v'/|\bar{V}_x|$ ranged from 6% to 18% one hour after the bore passage in August-September-October 2015 (Table 2). The horizontal turbulence ratio v_y'/v_x' was between 0.42 and 0.85, with the vertical turbulence ratio v_z'/v_x' being between 0.35 and 0.5. Such values were comparable to laboratory observations in straight prismatic rectangular channels (Nezu and Nakagawa, 1993; Nezu, 2005). Overall v_z'/v_x' was about two-thirds of the horizontal turbulence intensity v_y'/v_x' , and such a finding indicated some turbulence anisotropy during the flood tide motion behind the tidal bore.



(A) Water depth and longitudinal velocity component - Comparison between ADV data (sampling rate: 200 Hz) and surface velocity data



(B) Transverse and vertical velocity components

Figure 4. Water depth and instantaneous velocity data as functions of time during the Arcins channel tidal bore on 1 September 2015 for the entire data set

4 SUSPENDED SEDIMENT CHARACTERISTICS

The time-variations of the suspended sediment concentration (SSC) were deduced from the acoustic backscatter amplitude data, after a daily calibration. In addition, water samples were collected next to the surface before and after tidal bore (Fig. 5), and the data were analysed in laboratory subsequently. Typical data sets are presented in Figure 6 together with the water depth and the sediment concentrations of water samples. The SSC data showed some low SSC level at the end of the ebb tide: that is, $SSC < 2 \text{ kg/m}^3$ to 10 kg/m^3 typically. The passage of the tidal bore was associated with a very rapid increase in SSC levels together with large and rapid fluctuations in SSC estimates. Immediately after the bore, the water colour was dark brown, as seen in Figure 5. During the mid flood tide, the SSC estimates tended to decrease, about 30-45 minutes after the bore passage. For all field studies, maximum SSC levels were observed about 500-600 s after the bore passage, with maximum instantaneous SSC estimates up to $90\text{-}130 \text{ kg/m}^3$, while the water sample analysis yielded maximum SSCs larger than 60 kg/m^3 (Fig. 6B).

The SSC data, indicating some large sediment concentration during the tidal bore as well as during the first hour of the flood tide, were consistent with visual observations of murky water during the bore event. They were also comparable to previous field observations in several natural systems (Chanson et al., 2011; Fan et al., 2012; Keevil et al., 2015; Furgerot et al., 2016). All the field data highlighted the massive suspended sediment load after the tidal bore passage. Figure 7 regroups the present results by showing the time-average suspended sediment flux per unit area as a function of the time-average suspended sediment concentration for the first hour after the tidal bore. In Figure 7, the tidal bore data are compared to field data recorded in large rivers during major floods, including the Brisbane, Missouri and Yellow Rivers. The comparative results emphasised the large suspended sediment fluxes in the Garonne River tidal bore.

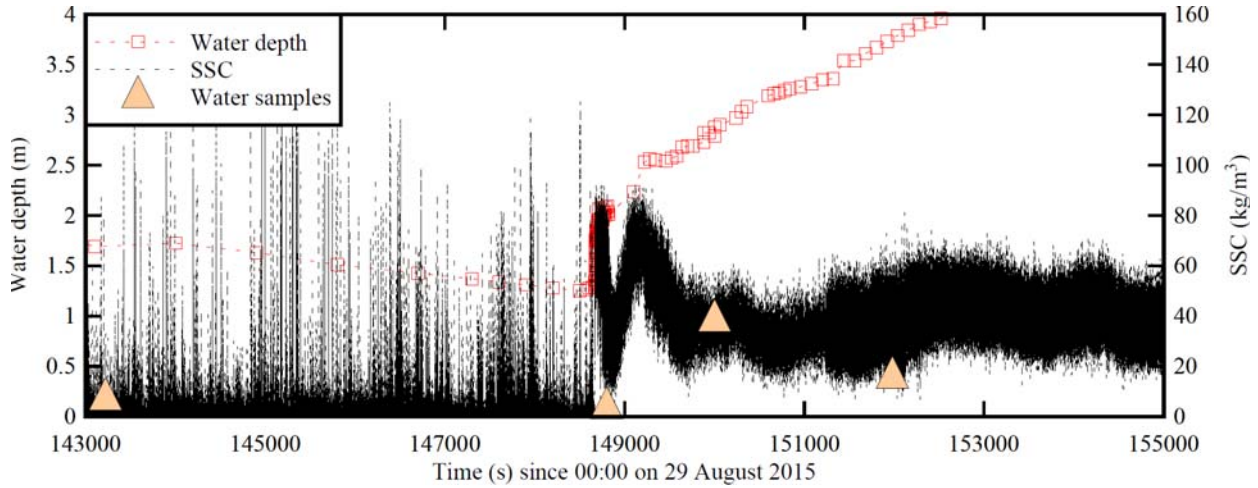
Table 2. Velocity properties in the Arcins channel immediately prior to, during and immediately after the tidal bore during the 2015 field measurements in the Arcins channel (Garonne River, France)

DATE	29/08/2015	30/08/2015	31/08/2015	01/09/2015	27/10/2015
Froude number Fr_1	1.18	1.34	1.70	1.38	1.33
Initial flow conditions					
Initial water depth (m) ⁽¹⁾	1.685	1.25	1.12	1.28	1.24
Initial surface velocity (m/s) ⁽²⁾	+0.29	+0.21	+0.18	+0.22	+0.22
Initial velocity \bar{V}_x (m/s) ⁽³⁾	+0.094	+0.105	+0.005	0.0	+0.066
Bore passage					
Maximum deceleration $(\partial \bar{V}_x / \partial t)_{\max}$ (m/s ²) ⁽³⁾	-1.2	-1.4	-0.883	-0.739	-0.645
Very early flood tide ($T_{\text{bore}}+20\text{s}$)					
\bar{V}_x (m/s) ⁽³⁾	-0.82	-0.83	-0.83	-0.84	-0.81
\bar{V}_y (m/s)	+0.02	-0.06	-0.06	-0.04	-0.06
\bar{V}_z (m/s)	-0.11	-0.14	-0.20	-0.22	-0.16
v_x' (m/s)	0.085	0.098	0.047	0.068	0.054
v_y' (m/s)	0.046	0.079	0.070	0.039	0.058
v_z' (m/s)	0.026	0.032	0.031	0.028	0.026
Early flood tide wave motion					
Time after bore passage (s)	180	170	170	175	50
Velocity amplitude V_x (m/s) ⁽³⁾	0.165	0.255	0.138	0.135	0.175
Velocity amplitude V_z (m/s)	0.10	0.11	0.102	0.07	0.10
Velocity oscillation period (s)	1.5	1.31	1.47	1.46	1.33
Flood tide ($T_{\text{bore}}+3600\text{s}$)					
\bar{V}_x (m/s) ⁽³⁾	-0.91	-1.02	-1.27	-0.90	-1.20
v_x' (m/s)	0.088	0.173	0.116	0.088	0.116
v_y' (m/s)	0.074	0.073	0.061	0.063	0.059
v_z' (m/s)	0.044	0.060	0.060	0.034	0.041

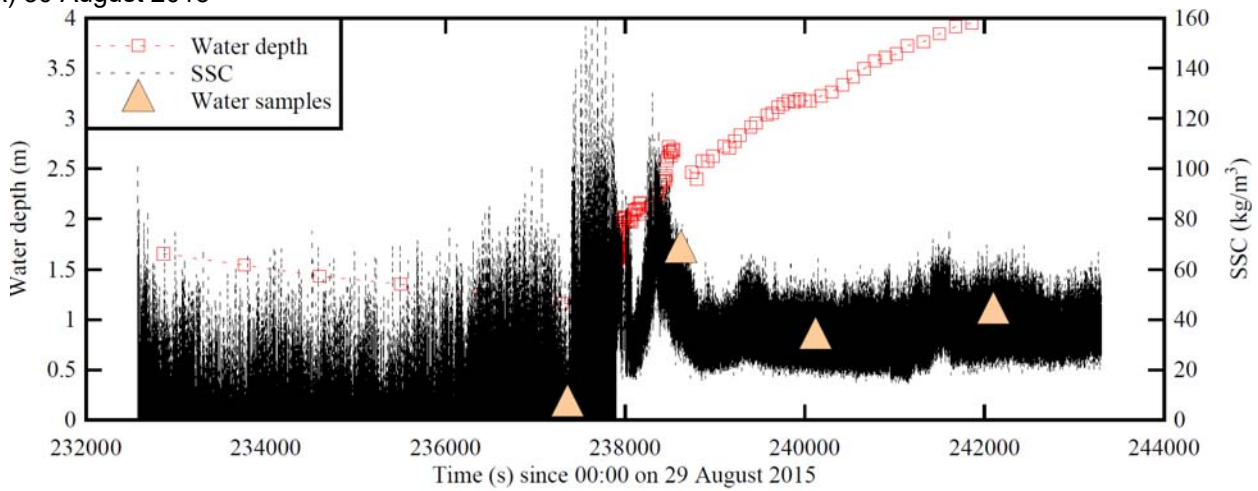
Notes: ⁽¹⁾: at survey staff; ⁽²⁾: surface data at channel centre; ⁽³⁾: ADV data.



Figure 5. Photograph of sediment-laden water samples collected on 27 October 2015 respectively at 14:00, 15:05 [before bore], 15:55, 15:59, 16:17 [after bore] (from right to left) - Tidal bore passage at 15:40- All samples were thoroughly mixed prior to the photograph



(A) 30 August 2015



(B) 31 August 2015

Figure 6. Suspended sediment concentration (SSC) and water depth data as functions of time during the Arcins channel tidal bore - Comparison between SSC estimates derived from ADV acoustic backscatter amplitude and water samples

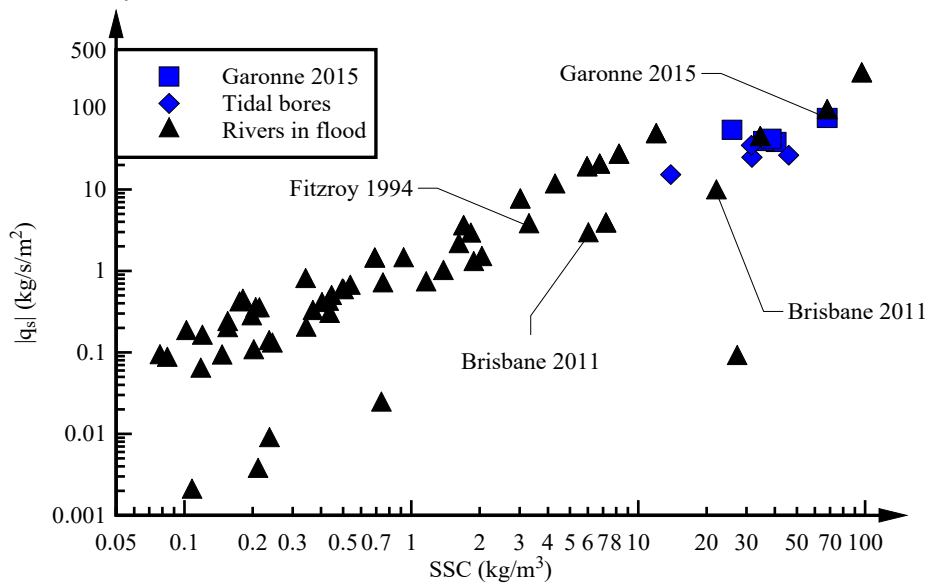


Figure 7. Time-average suspended sediment flux per unit area $\overline{q_s}$ ($\text{kg/m}^2/\text{s}$) as function of the mean time-average suspended sediment concentration $\overline{\text{SSC}}$ during the first hour of the flood tide after the tidal bore - Comparison between present tidal bore data (Garonne 2015, blue square symbols), past tidal bore data (blue diamond symbols) and observations of major flood river data (Amazon, Mississippi, Nile, Brisbane, Fitzroy and Yellow Rivers)

4.1 Discussion

Since 2010, the Arcins channel is believed to have experienced some progressive siltation (Keevil et al. 2015). In 2013, a build-up of low natural bar of hard materials was observed at the upstream end of the Arcins channel. In 2015, two low natural bars of relatively hard materials were noted, at both upstream and downstream ends of the channel. At the upstream end, the bar was established across the entire Arcins channel width: it was possible to walk to the Arcins Island in less than knee-deep waters. At the downstream end, surfers had barely enough water to surf the bore without damaging their board fins. At the sampling site, some siltation of both left and right banks was observed. It is conceivable that recent major floods of the Garonne River in 2012 and 2013 scoured the main river channel, west of the Arcins Island, thus reducing the flow into Arcins channel particularly at low tides and enhancing channel siltation.

5 CONCLUSION

The tidal bore of the Garonne River (France) was extensively investigated in the Arcins channel between 2010 and 2015. The 2015 field study aimed to comprehend the temporal evolution of hydrodynamics and sediment processes in a tidal bore affected estuarine zone during a spring tide period, by conducting comprehensive observations encompassing hydrodynamics, turbulence, and sediment transport.

The tidal bore had a marked effect on the velocity field, including a rapid flow deceleration and flow reversal during the bore passage, followed by large and rapid fluctuations of all velocity fluctuations during the early flood tide. The maximum flow deceleration ranged from -0.65 m/s^2 to almost -1.4 m/s^2 . The early flood flow motion was very energetic with large fluctuations of all velocity components. The suspended sediment concentration (SSC) data showed very large instantaneous SSC levels during the passage of the tidal bore front (in excess of 100 kg/m^3), as well as substantially large SSC estimates during the early flood tide for all the entire observations.

This study is the first detailed characterisation of turbulent sedimentary processes in a tidal bore affected channel with such a fine temporal and spatial resolutions: i.e., continuous sampling at 200 Hz in a small control volume $O(5 \text{ mm})$. The work culminates a 5-year research project at the same site, showing a progressive siltation of the Arcins channel during the last three years.

ACKNOWLEDGMENTS

The authors thank all the people who participated to the field works. They acknowledge the helpful inputs of Professor Pierre Lubin (University of Bordeaux, France). The financial assistance of the Agence Nationale de la Recherche (Projet Mascaret ANR-10-BLAN-0911) is acknowledged.

REFERENCES

- Chanson, H. (2011). *Tidal Bores, Aegir, Eagre, Mascaret, Pororoca: Theory and Observations*. World Scientific, Singapore, 220 pages (ISBN 9789814335416).
- Chanson, H. (2012). Momentum Considerations in Hydraulic Jumps and Bores. *Journal of Irrigation and Drainage Engineering*, ASCE, Vol. 138, No. 4, pp. 382-385 (DOI 10.1061/(ASCE)IR.1943-4774.0000409).
- Chanson, H., Reungoat, D., Simon, B., and Lubin, P. (2011). High-Frequency Turbulence and Suspended Sediment Concentration Measurements in the Garonne River Tidal Bore. *Estuarine Coastal and Shelf Science*, Vol. 95, No. 2-3, pp. 298-306 (DOI 10.1016/j.ecss.2011.09.012).
- Faas, R.W. (1995). Rheological Constraints on Fine Sediment Distribution and Behavior: The Cornwallis Estuary, Nova Scotia. *Proc. Can. Coastal. Conf.*, Dartmouth, Nova Scotia, pp. 301–314.
- Fan, D., Cai, G., Shan, S., Wu, Y., Zhang, Y., and Gao, L. (2012). Sedimentation processes and sedimentary characteristics of tidal bores along the north bank of the Qiantang Estuary. *Chinese Science Bulletin*, Vol. 57, No. 13, pp. 1578-1589 (DOI: 10.1007/s11434-012-4993-6).
- Furgerot, L., Mouaze, D., Tessier, B., Perez, L., Haquin, S., Weill, P., and Crave, A. (2016). Sediment transport induced by tidal bores. An estimation from suspended matter measurements in the Sée River (Mont-Saint-Michel Bay, northwestern France). *Comptes Rendus Géoscience*, Vol. 348, pp. 432-441 (DOI: 10.1016/j.crte.2015.09.004).
- Goring, D.G., and Nikora, V.I. (2002). Despiking Acoustic Doppler Velocimeter Data. *Journal of Hydraulic Engineering*, ASCE, Vol. 128, No. 1, pp. 117-126. Discussion: Vol. 129, No. 6, pp. 484-489.
- Greb, S.F., and Archer, A.W. (2007). Soft-Sediment Deformation Produced by Tides in a Meizoseismic Area, Turnagain Arm, Alaska. *Geology*, Vol. 35, No. 5, pp. 435-438.
- Keevil, C.E., Chanson, H., and Reungoat, D. (2015). Fluid Flow and Sediment Entrainment in the Garonne River Bore and Tidal Bore Collision. *Earth Surface Processes and Landforms*, Vol. 40, No. 12, pp. 1574-1586 (DOI: 10.1002/esp.3735).
- Khezri, N., and Chanson, H. (2015). Turbulent Velocity, Sediment Motion and Particle Trajectories under Breaking Tidal Bores: Simultaneous Physical Measurements. *Environmental Fluid Mechanics*, Vol. 15, No. 3, pp. 633-651 (DOI: 10.1007/s10652-014-9358-z) & (DOI: 10.1007/s10652-014-9360).

- Nezu, I. (2005). Open-Channel Flow Turbulence and its Research prospect in the 21st Century. *Journal of Hydraulic Engineering*, ASCE, Vol. 131, No. 4, pp. 229-246.
- Nezu, I., and Nakagawa, H. (1993). *Turbulence in Open-Channel Flows*. IAHR Monograph, IAHR Fluid Mechanics Section, Balkema Publ., Rotterdam, The Netherlands, 281 pages.
- Reungoat, D., Chanson, H., and Caplain, B. (2014). Sediment Processes and Flow Reversal in the Undular Tidal Bore of the Garonne River (France). *Environmental Fluid Mechanics*, Vol. 14, No. 3, pp. 591-616 (DOI: 10.1007/s10652-013-9319-y).
- Reungoat, D., Leng, X., and Chanson, H. (2016). Hydrodynamic and Sedimentary Processes of Tidal Bores: Arcins Channel, Garonne River in August-September-October 2015. *Hydraulic Model Report No. CH102/16*, School of Civil Engineering, The University of Queensland, Brisbane, Australia, 270 pages (ISBN 978-1-74272-155-2).
- Tanaka, N., Yagisawa, J., and Yasuda, S. (2012b). Characteristics of Damage due to Tsunami Propagation in River Channels and Overflow of their Embankments in Great East Japan Earthquake. *International Journal of River Basin Management*, Vol. 10, No. 3, pp. 269-279.
- Tricker, R.A.R. (1965). *Bores, Breakers, Waves and Wakes*. American Elsevier Publ. Co., New York, USA.
- Wahl, T.L. (2003). Despiking Acoustic Doppler Velocimeter Data. Discussion. *Journal of Hydraulic Engineering*, ASCE, Vol. 129, No. 6, pp. 484-487.